

Imaging of the anterior segment of the eye by spectral optical coherence tomography

JAKUB J. KAŁUŻNY

Department of Ophthalmology, The Ludwik Rydygier's University School of Medical Science, ul. Marii Skłodowskiej-Curie 9, 85-094 Bydgoszcz, Poland.

MACIEJ WOJTKOWSKI, ANDRZEJ KOWALCZYK

Institute of Physics, Nicholas Copernicus University, ul. Grudziądzka 5, 87-100 Toruń, Poland.

Spectral optical coherence tomography (SOCT) is a new imaging modality competitive to the well-known temporal optical coherence tomography (OCT) systems. This technique is based on direct measurements of the spectral fringe pattern, obtained by interference of the light scattered back from a tissue and the light reflected from a reference mirror. We present first tomographic images of the cornea, anterior angle and iris obtained by SOCT. The advantages as well as the artifacts of the method are discussed.

1. Introduction

The detection of the light scattered back from an object, illuminated by the light of low temporal but high spatial coherence, is the basis of the optical coherence tomography (OCT). During the last decade of the twentieth century OCT has been developed and at present is an important diagnostic technique in medicine. The success of OCT lies in the micron longitudinal resolution, high sensitivity, precision and non-contact operation. The most advanced applications of OCT are in ophthalmology, for example, in high-resolution imaging of the anterior chamber of the eye [1]–[3], in determining the thickness of a nerve fiber layer, in establishing the topography of the optic disc [4] and in macular morphology [5]–[7] which are the most desirable parameters for detection, quantification and monitoring of macular degeneration and glaucoma. OCT has been proposed as an alternative method for biometry, allowing to determine the intraocular distances more precisely than ultrasounds. Recently, some studies has confirmed the high accuracy and reproducibility of corneal thickness measurements performed with the use of OCT [8]–[11].

The more advanced application of OCT is the development of functional OCT. It has been achieved due to spectroscopically sensitive techniques which enable us to obtain the absorption spectrum of a tissue at the given depth. This piece of information can be related to the hemoglobin concentration (total, oxyhemoglobin,

deoxyhemoglobin) or to the concentration of external substances (*e.g.*, eye drops) possessing a strong absorption in this wavelength range. Therefore, such issues as blood oxygenation in inaccessible tissues, *e.g.*, in the fundus, or various problems of pharmacokinetics can now be addressed. The first results of spectroscopically sensitive OCT were reported in 2000 [12], [13]. OCT combined with the Doppler phenomenon demonstrates the ability to quantitative blood flow imaging [14]. The polarization sensitive OCT detects changes induced in the polarization state of light which is reflected from a birefringent sample, such as muscle or retina, and enhances contrast and specificity while identifying these structures.

There are several competitive techniques which provide tomographic sections of the eye *in vivo*. The ultrasound biomicroscopy (UBM) uses ultrasound waves at the frequency of 50–100 MHz providing the resolution ranging from 20 to 60 μm with the penetration depth of approximately 4 mm [15]. The examination is performed in real time. Because ultrasound penetrates also opaque media, shadowing of the anterior chamber angle does not exist and good quality images of the anterior segment together with the ciliary body and peripheral retina can be obtained [16]–[19]. Magnetic resonance (MR) is the other technique which can be used for the examination of the anterior segment *in vivo*. Although MR is a valuable tool in a diagnosis of orbit diseases, the structures of the globe are reproduced rather poorly. Employing special coils enables us to achieve the maximum resolution of about 200 μm with an acquisition time of several minutes per sequence [20].

There are two implementations of OCT depending on the kind of used detectors: historically the first one is the time domain OCT (TdOCT), where the detection is time dependent, and the second one is SOCT developed later, where the signal is detected as a function of optical frequencies. In SOCT the detection is realised by a spectrometric system. It provides direct access to spectral and phase information, what renders the spectral technique advantageous in comparison with temporal OCT. While the TdOCT systems are used in clinical practice (commercially available: OCT 1,2,3 Carl Zeiss Ophthalmic Systems Inc's Humphrey Div.), the SOCT devices are still in the prototype phase. To our knowledge, images of the cornea, anterior angle and iris have not been obtained by SOCT to date.

2. Material and methods

Anterior segment measurements were performed on three healthy volunteers, aged 25–33 years, without any previously reported eye or general disease. One subject wore soft contact lenses because of small myopia.

SOCT images were generated by a system developed in the Institute of Physics, Nicholas Copernicus University, Toruń, Poland. A detailed description of the instrument and the method may be found elsewhere [21]. Briefly, the interferometer, the main part of the SOCT instrument, is based on an open air Michelson interferometer set-up (Fig.1a) with a 50/50 cube beam splitter. A superluminescent diode is a light source emitting at a wavelength of 810 nm with a 20 nm FWHM and

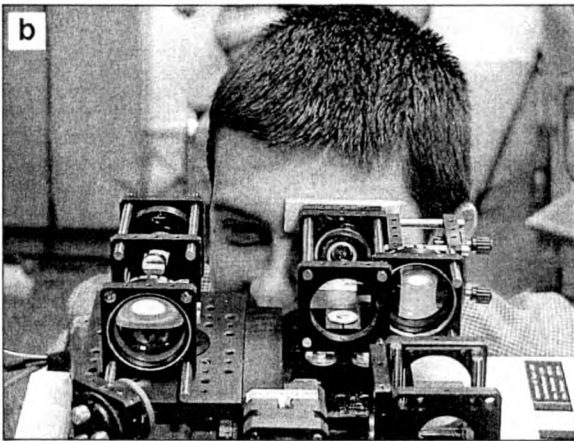
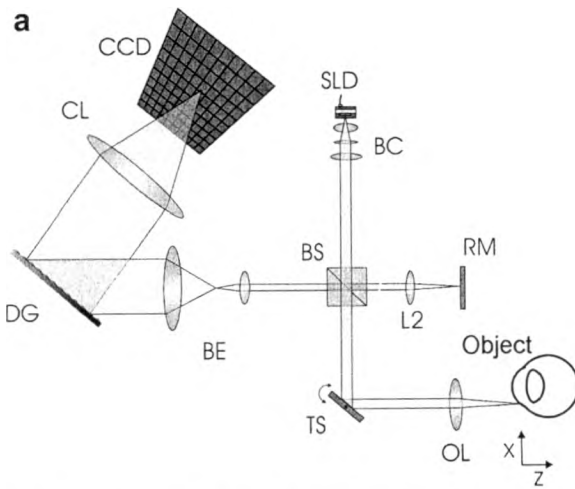


Fig. 1. Fourier domain spectral OCT device. **a** – optical scheme (SLD – superluminescent diode, BC – collimator, RM – reference mirror, BS – beam splitter, OL – objective lens, L2 – lens, TS – transversal scanner, BE – beam expander, DG – diffraction grating, CL – camera objective, CCD – camera); **b** – photography of the device during the measurement.

a maximal output power of 2 mW. An object arm of the interferometer is used both for illuminating the eye and for collecting the reflected light. The information about the distribution of reflecting layers in the object along an illuminating beam is extracted from a spectral fringes pattern registered by a spectrometer consisting of a diffraction grating (1800 grooves/mm) and a CCD camera. The detected signal is digitalized and transferred to the personal computer (1 MHz sampling rate of 16 bit AD conversion).

One dimensional A-scan profile of optical reflectivity *vs.* optical distance inside the eye is created by the numerical Fourier transformation (FFT) of the spectral fringes pattern. Time needed to register one spectral fringes profile is equal

to 128 μ s. The transfer time of 128 spectral fringes profiles between CCD and PC takes 160 ms. The data are processed and visualized by a software written in LabView.

The images of sections through the cornea, sclera, chamber angle and iris were performed for each patient. The measurements were carried out in sitting position. Neither topical application of anesthetics nor speculum insertion were necessary for the examination. The aiming was done by observing a beam with an infrared camera. In our system the probe spot was created by the lens (OL), focal length $f = 25.4$ mm, mounted in front of the eye. An initial optical path difference was achieved adjusting the patient's head in a chin rest. The scanning mirror ensured lateral beam positioning. Both the focal depth of the object lens and the spectral resolution of the spectrometer determine the measurement range of the spectral OCT device and in our instrument it is designed to be 1.5 mm. The size of the probe spot determines the transversal resolution which is approximately $\Delta x = 25$ μ m. The optical power of the incident beam at the cornea is $P = 23$ μ W (this value is consistent with the PN-91/T-06700 recommended exposure limit for CW direct beam viewing) [22].

On average, 5 to 10 images of each structure with different incident angles of a sample beam were recorded and further examined.

3. Results

Figure 2 shows the image of the section of the human cornea *in vivo* taken without (a), and with (b) a soft lens on top of it. The shape of air/cornea and air/contact lens surfaces are sharply reproduced with the accuracy of tens micrometers. The contact lens is optically transparent and homogenous, therefore no back reflected light is registered from its inside. The cornea is transparent but due to its fibrous structure light scatters at these fibers producing a weak background signal originating from the stroma. The image shows an apparent internal structure of the cornea, namely two stripes of enhances reflection at the upper and lower border of the cornea,

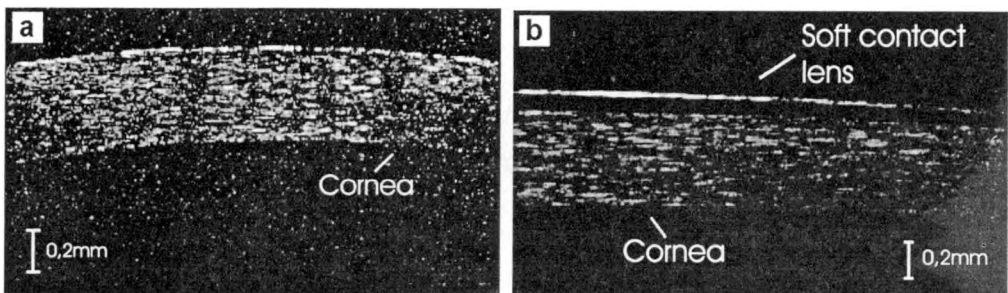


Fig. 2. SOCT cross-sectional images: a – human cornea *in vivo*, b – human cornea with a soft contact lens on the surface *in vivo*.

which may be attributed to corneal epithelium and Bowman membrane, as well as to corneal endothelium and Descemet membrane, respectively. Such structures were observed by other authors [1]–[3]. More probable, however, is that this signal originates from the strong reflection at the air/cornea interface due to the rapid change of the refractive index. Indeed, when a soft contact lens was applied, the layer of increased reflectivity at the anterior surface of the cornea disappeared together with a false stripe at the anterior surface of the cornea.

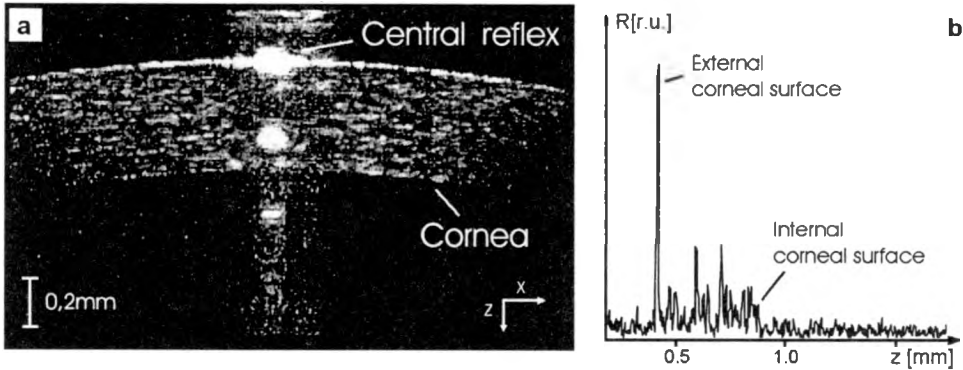


Fig. 3. SOCT of the central part of the human cornea: **a** – cross-sectional image, **b** – A-scan of the area situated near the central reflex point.

Figure 3a presents a cross-sectional image of the central part of the human cornea *in vivo*. A characteristic vertical stripe indicating very high reflectivity at the center of the cornea results from the fact that light beam direction of incidence is exactly perpendicular to the corneal surface at that point. Therefore, close to this point, the measurement of the corneal optical thickness, without any additional corrections arising from refraction, is possible. In order to estimate the corneal optical thickness, axial intensity distribution is taken from the place situated near to the central reflex point (Fig. 3b). The estimated optical corneal thickness at this point is $d = 0.75$ mm.

Figures 4a,b,c show tomographic images of the anterior chamber region of the human eye *in vivo* taken with three different orientations of the eye with respect to the direction of the probing beam. The irregular structure of collagen bundles arranged in an irregular fashion makes the sclera opaque. The sclera scatters so strongly that sensitivity of the detector has to be reduced. Under these conditions the background from the inside of the cornea is not visible in the image. It seems that the thin layer of lower reflectivity on the scleral surface corresponding to the conjunctiva can be resolved but, as in the previous case, it might be confused with a strong reflection on the air interface. Due to scleral nontransparency the structures laying deeper, like *pars plicata* and *pars plana* of the ciliary body, could not be observed. The place where an irregular structure of collagen fibers changes for a regular corneal pattern is clearly visible (corneo-scleral junction). Although the basic

morphology of the anterior chamber is evident on the OCT image, the accurate evaluation of details of this angle is difficult. The peripheral part of the iris and the apex of the anterior chamber angle are shadowed by the anteriorly located sclera. This part of the angle plays an important role in the classification of the angle and in estimating the risk of acute angle glaucoma. The second issue involves distortion of

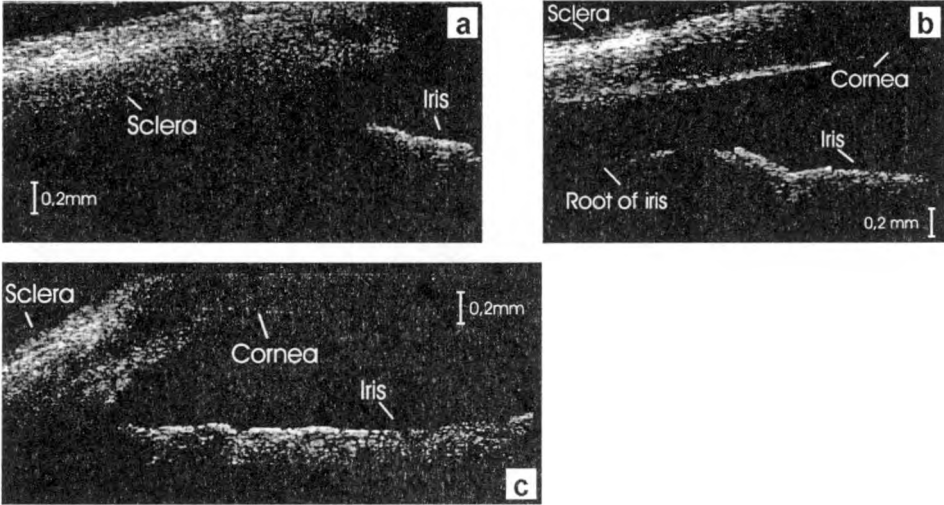


Fig. 4. SOCT of the anterior chamber angle: a – incident beam is directed obliquely from the scleral side, b – incident beam runs obliquely from the corneal side, c – incident beam is perpendicular to the corneal surface.

the angle images as a result of corneal refraction which appears when the sample beam is not perpendicular to the corneal surface. If the incident OCT beam is directed obliquely from the scleral side, the angle is wider (Fig. 4a). Apex of the angle is more visible when the sample beam runs at an angle from the corneal side. In this situation the angle seems narrower (Fig. 4b). For an accurate analysis of the anterior chamber width the mathematical correction of this distortion is necessary.

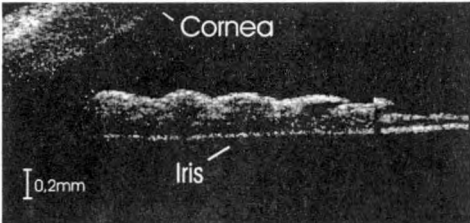


Fig. 5. SOCT tomographic cross-section of the iris.

Figure 5 shows a tomographic section through the iris of the human eye *in vivo*. The iris section, especially its pupil margin, is well reproduced. The iris root,

a place where the iris is connected to the anterior part of the ciliary body, is shadowed by the sclera and it is not imaged under these conditions.

Three distinct layers can be observed in the section. The most anterior layer of intensive reflectivity may correspond to the anterior part of the iris stroma, which has an irregular surface of *trabeculae* and *crypts*. This structure is rich in pigment, which is a highly scattering medium for light. The much lower reflectivity is typical for the rest of the stroma. The most internal part of the iris is pigment epithelium which consist of two layers of cells rich in melanin. On OCT images it appears as a distinct layer of slightly increased reflectivity. Fibers of the pupil constrictor and dilatator, as well as vascular vessels within iris stroma, are not revealed with this technique.

4. Discussion

We have demonstrated the SOCT potential to perform ophthalmological tomograms for humans *in vivo*. This technique makes it possible to obtain cross-sectional images of structures *in vivo* with a spatial resolution less than 20 μm in relatively short time, to decrease motion artifacts and increase the patient's comfort.

SOCT produces sharp images of the anterior and posterior surface of the cornea and can be used for an evaluation of the corneal optical thickness. However, reliable measurements can be obtained only in the central region, where a sample beam is perpendicular to the surface. In order to obtain real geometrical dimensions the optical distances should be divided by the index of refraction. Moreover, for oblique beam direction the resulting images are distorted and must be corrected for refraction at the air-cornea interface. It is important for pachymetric evaluation of the corneal thickness and even more crucial for the determination of anterior angle geometry. Although the structure of the cornea is not revealed, its surface is well reproduced. Therefore SOCT can be applied to an evaluation of a corneal shape and structure after repetitive surgery and penetrating keratoplasty, as well as to an estimation of the quality of contact lens fitting and their influence on the corneal metabolism. It can be also helpful in diagnosis of different corneal diseases and degenerations.

The quality of presented images seems to be sufficient for diagnosis of iris tumors and post traumatic changes of the anterior chamber and for an evaluation of structural causes of different types of glaucoma such as angle closure glaucoma and pupillary block glaucoma. This technique can be also useful in assessing the effect of glaucoma surgery. However, for the latter, the OCT at longer wavelength (1310 nm) would give more accurate results [3], [23].

In SOCT a direct contact between the probe and the globe is not required. The examination is fast and not annoying for the patient. It is worth mentioning that no special preparation or topical anesthesia is necessary.

However, there are two disadvantages of OCT. The first one is that in this method we cannot obtain images through opaque media impairing visualization of

the anterior chamber and ciliary body [1]–[3], [23]. The second one is the necessity of the correction for refraction if true geometrical distances are required.

The other existing methods such as UBM and MR have an essential advantage of the ability to produce tomograms of opaque tissues. However, UBM requires a direct contact between the probe and the globe surface through coupling medium. The examination is always performed in supine position and requires topical anesthesia. This entire procedure is highly unpleasant for the patient. Due to a relatively low resolution and a high number of artifacts, the detection of lesions smaller than 2 mm is very difficult in MR [24]. In spite of the fact that all the structures of the anterior segment are visible, an accurate evaluation of the corneal thickness or anterior chamber angle using the currently available MR systems cannot be achieved in a routine examination.

We can conclude that SOCT is an important tool for an evaluation of the anterior segment. The examination can be easily performed in a way convenient for the patient. The list of possible applications is long and probably will be soon extended thanks to new opportunities given by this technique.

Acknowledgments – The authors, M.W. and A.K., are grateful for financial support from the State Committee for Scientific Research (KBN), Poland, Grant No. 4T11E02322, and UMK Grant No. 502-F.

References

- [1] HOERAUF H., BIRNGRUBER R., [In] *Handbook of Optical Coherence Tomography*, [Eds.] B.E. Bouma, G.J. Tearney, Dekker, New York 2002.
- [2] HOERAUF H., WIRBELAUER C., SCHOLZ C., ENGELHARDT R., KOCH P., LAQUA H., BIRNGRUBER R., *Graefe's Arch. Clin. Exp. Ophthalmol.* **238** (2000), 8.
- [3] RADHAKRISHNAN S., ROLLINS A.M., ROTH J.E., YAZDANFAR S., WESTPHAL V., BARDENSTEIN D.S., IZATT J.A., *Arch. Ophthalmol.* **119** (2001), 1179.
- [4] ZANGWILL L.M., BOWD C., BERRY C.C., WILLIAMS J., BLUMENTHAL E.Z., SANCHEZ-GALEANA C.A., VASILE C., WEINREB R.N., *Arch. Ophthalmol.* **119** (2001), 985.
- [5] GALLEMORE R.P., JUMPER J.M., MCCUEN B.W., II, JAFFE G.J., POSTEL E.A., TOTH C.A., *Retina* **20** (2000), 115.
- [6] GIOVANNINI A., AMATO G., MARIOTTI C., SCASELLATI-SFORZOLINI B., *ibidem*, p. 37.
- [7] HEE M.R., PULIAFITO C.A., DUKER J.S., REICHEL E., COKER J.G., WILKINS J.R., SCHUMAN J.S., SWANSON E.A., FUJIMOTO J.G., *Ophthalmol.* **105** (1998), 360.
- [8] BÖHNKE M., MASTERS B.M., WÄLTI R., BALLIF J.J., CHAVANNE P., GIANOTTI R., SALATHÉ R.P., *J. Biomed. Opt.* **4** (1999), 152.
- [9] WANG J., FONN D., SIMPSON T.L., JONES L., *Am. J. Ophthalmol.* **134** (2002), 93.
- [10] WIRBELAUER C., SCHOLZ C., HOERAUF H., PHAM D.T., LAQUA H., BIRNGRUBER R., *Am. J. Ophthalmol.* **133** (2002), 444.
- [11] BECHMANN M., THIEL M.J., NEUBAUER A.S., ULLRICH S., LUDWIG K., KENYON K.R., ULBIG M.W., *Cornea* **20** (2001), 50.
- [12] MORGNER U., DREXLER W., KÄRTNER F.X., LI X.D., PITRIS C., IPPEN E.P., FUJIMOTO J.G., *Opt. Lett.* **25** (2000), 111.
- [13] LEITGEB R., WOJTKOWSKI M., HITZENBERGER C.K., STICKER M., KOWALCZYK A., FERCHER A.F., *ibidem*, p. 820.
- [14] DING Z., ZHAO Y., REN H., NELSON J.S., CHEN Z., *Optics Express* **10** (2002), 236.
- [15] PAVLIN C.J., HARASIEWICZ K., SHERAR M.D., FOSTER F.S., *Ophthalmol.* **98** (1991), 287.

- [16] MARIGO F.A., FINGER P.T., MCCORMICK S.A., IEZZI R., ESAKI K., SIHAWA H., LEIBMANN J.M., RITCH R., *Arch. Ophthalmol.* **118** (2000), 1515.
- [17] MANNINO G., MALAGOLA R., SOLMAZ A., VILANI G.M., RECUPERO S.M., *Br. J. Ophthalmol.* **85** (2001), 976.
- [18] KOBAYASHI H., ONO H., KIRYU J., KOBAYASHI K., *Br. J. Ophthalmol.* **83** (1999), 559.
- [19] KOBAYASHI H., HIROSE M., KOBAYASHI K., *Br. J. Ophthalmol.* **84** (2000), 1142.
- [20] HOSTEN N., LEMKE A.J., SANDER B., WASSMUTH R., TERSTEGGE K., BORNSFIELD N., FELIX R., *Eur. Radiol.* **7** (1997), 459.
- [21] WOJTKOWSKI M., KOWALCZYK A., TARGOWSKI A., GORCZYŃSKA I., *Opt. Appl.* **32** (2002), 569.
- [22] Polish Standards: PN-91/T-06700.
- [23] HOERAUF H., GORDES R.S., SCHOLZ C., WIRBELAUER C., KOCH P., ENGELHARDT R., WINKLER J., LAQUA H., BRINGRUBER R., *Ophthalmic Surg. Lasers* **31** (2000), 218.
- [24] MAFEE M.F., PEYMAN G.A., GRISOLANO J.E., FLETCHER M.E., SPIGOS D.G., WEHRLI F.W., RASOULI F., CAPEK V., *Radiology* **160** (1986), 773.

*Received July 19, 2002
in revised form September 30, 2002*